EUROPEAN ORGANIZATION FOR NUCLEAR RESEARCH

CERN-EP/99-024
February 18, 1999

Search for Scalar Leptons in e^+e^- collisions at $\sqrt{s} = 183$ GeV

The L3 Collaboration

Abstract

We report the result of a search for scalar leptons in e^+e^- collisions at 183 GeV centre-of-mass energy at LEP. No evidence for such particles is found in a data sample of 55.2 pb^{-1}. Improved upper limits are set on the production cross sections for stable as well as unstable scalar leptons. New exclusion contours in the parameter space of the Minimal Supersymmetric Standard Model are derived, as well as new lower limits on scalar lepton masses.

Submitted to *Phys. Lett. B*

1 Introduction

One of the main goals of the LEP experiments is to search for new particles predicted by theories beyond the Standard Model. In this letter we report on searches for stable and unstable scalar leptons. Scalar leptons naturally occur in supersymmetric theories (SUSY) [1]. In SUSY theories with minimal particle content (MSSM) [2], in addition to the ordinary particles, there is a supersymmetric spectrum of particles with spins which differ by one half with respect to their Standard Model partners. Scalar leptons ($\tilde{\ell}^{\pm}_R$ and $\tilde{\ell}^{\pm}_L$) are the supersymmetric partners of the right- and left-handed leptons. They are produced in pairs through s-channel γ/Z exchange. For scalar electrons the production cross section is enhanced by t-channel exchange of a neutralino.

Long-lived scalar leptons are expected in Gauge Mediated SUSY Breaking (GMSB) models [3] as well as in R-parity violating SUSY models [4]. The R-parity is a quantum number which distinguishes ordinary particles from supersymmetric particles. In GMSB, if the scalar lepton is the next-to-lightest supersymmetric particle, it may acquire a long lifetime for high SUSY-breaking energy scales [5]. For small R-parity violating couplings ($\lambda < 3 \cdot 10^{-9}$), decay lengths longer than ten meters are predicted at LEP energies whenever the scalar lepton is the lightest supersymmetric particle, thus leading to a "stable" heavy lepton signature.

Short-lived scalar leptons are expected in R-parity conserving SUSY models. If R-parity is conserved supersymmetric particles are pair-produced and the lightest supersymmetric particle, the neutralino $\tilde{\chi}^0_1$, is stable. The neutralino is weakly-interacting and escapes detection. The scalar lepton decays into its partner lepton mainly via $\tilde{\ell}^{\pm} \rightarrow \tilde{\chi}^0_1 \ell^{\pm}$, but also via the cascade decay, such as $\tilde{\ell}^{\pm} \rightarrow \tilde{\chi}^0_2 \ell^{\pm} \rightarrow \tilde{\chi}^0_1 \mathrm{Z}^* \ell^{\pm}$, which may dominate in some regions of the parameter space of the MSSM.

Results are presented here of a search for scalar leptons at centre-of-mass energies up to 182.7 GeV. Previous limits on scalar leptons have been reported by L3 [6] and other LEP experiments [7]. In this paper, model independent limits are presented on production cross sections, and are interpreted in terms of MSSM parameters. These limits are obtained by combining the results of the present search with those obtained previously by L3 [6, 8].

2 Data sample and simulation

We present the analysis of data collected by L3 [9] in 1997, corresponding to an integrated luminosity of 55.2 pb^{-1} at an average centre-of-mass energy of 182.7 GeV, denoted hereafter as 183 GeV. The search for stable scalar leptons also includes data collected at the following centre-of-mass energies: $130 - 136$ GeV (12.1 pb^{-1}) and $161 - 172$ GeV (21.1 pb^{-1}).

Events from Standard Model reactions are simulated with the following Monte Carlo generators: `PYTHIA` [10] for $\mathrm{e}^+\mathrm{e}^- \rightarrow \mathrm{q\bar{q}}$, $\mathrm{e}^+\mathrm{e}^- \rightarrow \mathrm{Z\,e^+e^-}$ and $\mathrm{e}^+\mathrm{e}^- \rightarrow \gamma/\mathrm{Z}\,\gamma/\mathrm{Z}$; `EXCALIBUR` [11] for $\mathrm{e}^+\mathrm{e}^- \rightarrow \mathrm{W}^{\pm}\,\mathrm{e}^{\mp}\nu$; `KORALZ` [12] for $\mathrm{e}^+\mathrm{e}^- \rightarrow \mu^+\mu^-$ and $\mathrm{e}^+\mathrm{e}^- \rightarrow \tau^+\tau^-$; `BHAGENE3` [13] for $\mathrm{e}^+\mathrm{e}^- \rightarrow \mathrm{e}^+\mathrm{e}^-$; `KORALW` [14] for $\mathrm{e}^+\mathrm{e}^- \rightarrow \mathrm{W}^+\mathrm{W}^-$; `DIAG36` [15] for $\mathrm{e}^+\mathrm{e}^- \rightarrow \mathrm{e}^+\mathrm{e}^-\ell^+\ell^-$ and `PHOJET` [16] for $\mathrm{e}^+\mathrm{e}^- \rightarrow \mathrm{e}^+\mathrm{e}^-$ hadrons. For the last two processes, events are simulated only for two-photon invariant masses above 3 GeV. The number of events for each simulated background process is at least 100 times that of the collected data sample, except for two-photon interactions for which it is more than two times the collected data.

Signal events are generated with the Monte Carlo program `SUSYGEN` [17], for masses of scalar leptons ($M_{\tilde{\ell}^{\pm}}$) ranging from 45GeV up to the kinematic limit and for ΔM values ($\Delta M = M_{\tilde{\ell}^{\pm}} - M_{\tilde{\chi}^0_1}$) between 3 GeV and $M_{\tilde{\ell}^{\pm}} - 1$ GeV.

The detector response is simulated using the GEANT package [18]. It takes into account effects of energy loss, multiple scattering and showering in the detector materials and in the beam pipe. Hadronic interactions are simulated with the GHEISHA program [19]. Time dependent inefficiencies of the different subdetectors are also taken into account in the simulation procedure.

3 Search procedure for stable scalar leptons

Pair production of long-lived heavy scalar leptons appears as two back-to-back charged tracks in the detector. As the mass of the scalar lepton increases, the differential energy loss (dE/dx) increases, while the available kinetic energy decreases. For masses up to about 80% of the beam energy (E_B), the heavy lepton has sufficient kinetic energy to penetrate both the electromagnetic (BGO) and hadronic calorimeters, and makes a track in the muon chambers.

The analysis is designed for stable particle masses in the range between 45 GeV and the beam energy. To reject backgrounds from pair production of light particles, the search uses both the dE/dx information from the tracking chamber and the muon chamber momentum measurement. The search is performed with selection requirements optimised in three different mass regions: high ($M/E_B > 0.8$), intermediate ($0.7 < M/E_B < 0.8$) and low ($0.5 < M/E_B < 0.7$).

Events are selected which have two charged tracks with momentum greater than 5 GeV and polar angle $|\cos\theta| < 0.82$. The acollinearity angle between the two tracks is required to be less than $15°$. The polar angle requirement selects events where the trigger and track reconstruction efficiency is high and the dE/dx resolution is good. From independently-triggered $e^+e^- \rightarrow e^+e^-$ events, the tracking chamber trigger efficiency is determined to be 98% over the interval $|\cos\theta| < 0.82$. The momentum and acollinearity angle requirements reduce the backgrounds from lepton pairs produced in two-photon collisions or in association with a high energy photon. After these requirements 4503 events are selected in data with 4410 expected from Standard Model processes, mainly from $e^+e^- \rightarrow e^+e^-$.

3.1 High mass region

In the region $M/E_B > 0.8$, only the tracking chamber information is utilised. Ionization energy loss is measured in units of minimum ionising particles. The dE/dx measurement is calibrated with Bhabha scattering events, and the resulting dE/dx resolution is $\sigma_{\mathrm{dE/dx}} = 0.08$. Events are selected for which the ionization energy loss for each track is between 1.25 and 8, and the product of the track ionization losses is larger than 2.

Figure 1 shows dE/dx for the first and second track for data events passing all cuts except those on track ionization. In Figure 1 is also shown the simulated signal from pair-production of heavy scalar leptons at 183 GeV. No events are observed in the region defined by the dE/dx cut in this sample or in any of the lower energy samples.

In order to estimate background contamination, a control sample of 30 pb^{-1} of data collected at the Z peak is used. The fraction of Z events which have both tracks in the signal region is less than 4×10^{-5} at 90% C.L., which leads to an estimated background of less than 0.2 events in the combined $130 - 183$ GeV data.

The efficiency for selection of stable scalar leptons ranges from 80% to 86% over the mass range $0.8 < M/E_B < 0.99$. At very high masses, the charged particles are highly ionising and saturation effects become significant, which may lead to track reconstruction inefficiencies.

3.2 Intermediate mass region

In the region $0.7 < M/E_B < 0.8$, the dE/dx signature is insufficient to reject the backgrounds from lighter particles. Assuming the heavy scalar leptons live long enough to traverse the entire L3 detector, then they have sufficient kinetic energy to penetrate the calorimeters and produce a high momentum track in the muon chambers. Events are required to satisfy the following criteria: the matched energy deposit in the BGO is less than 2 GeV for each track; the ionization energy loss for each track is greater than 1.05 and their product is larger than 1.25; and there is at least one muon track with $P_\mu/E_B > 0.4$.

No such events are observed in any of the data samples. The total background in the full $130-183$ GeV data is estimated to be 0.5 events. The selection efficiency ranges from 50% at $M/E_B = 0.7$ up to 80% at $M/E_B = 0.8$.

3.3 Low mass region

In the region $0.5 < M/E_B < 0.7$, the dE/dx is indistinguishable from that of lighter particles. Consequently, only the muon chamber momentum and calorimeter information are used. Assuming the energy of the particles is E_B, the momentum of the muon track is used to reconstruct the mass of the particle. Events are required to satisfy the following criteria: two tracks are found in the muon spectrometer in the polar angle range $|\cos\theta| < 0.76$, each with $0.5 < P_\mu/E_B < 1.0$; the acollinearity angle between the tracks is less than 10°; the matched energy deposit in the BGO is less than 2 GeV for each track; the sum of the unmatched BGO energy deposits is less than 1 GeV. In addition, there is at least one time-of-flight counter time within 5 ns of the beam crossing time. The reconstructed mass of each particle exceeds 45 GeV.

No events pass the selection requirements in any of the data samples. From the Monte Carlo, the background is estimated to be 0.7 events in the entire $130-183$ GeV data sample. The selection efficiency for scalar leptons ranges from 14% at $M/E_B = 0.5$ up to 45% at $M/E_B = 0.7$.

4 Search procedure for unstable scalar leptons

In R-parity conserving models we expect two undetected $\tilde{\chi}^0_1$ in the final state for all processes. Therefore the signature of scalar lepton production is the following: two acoplanar leptons, large missing transverse momentum, missing energy, and missing mass. To account for the three lepton families, three different selections are performed.

The signal topologies and the associated background sources depend strongly on the visible energy, which is approximately proportional to ΔM ($\Delta M = M_{\tilde{\ell}^\pm} - M_{\tilde{\chi}^0_1}$). Therefore each of the three selections is optimised for three different ΔM ranges: low ($3-10$ GeV), medium ($20-30$ GeV) and high ($60-80$ GeV). In the low ΔM range the expected signal is characterised by low visible energy, and the background is dominated by two-photon interactions. In the highest ΔM range the main background is due to leptonic W decays.

Events are preselected as described in Reference 6. Distributions at the preselection level, for data and Monte Carlo at 183 GeV, for the most important variables of scalar lepton selections are shown in Figure 2. The variables shown are E_{TLT}, which is defined as the absolute value of the projection of the total momentum of the two leptons onto the direction perpendicular to the leptonic thrust computed in the R-ϕ plane; and the normalised transverse energy, E_{TL}, of the two leptons. Good agreement is observed between data and expected background. Simulated signal distributions are also shown for comparison.

The selections are optimised using the same procedure and variables described in Reference 6. The optimised cut values are tighter than those in Reference 6 due to the increased integrated luminosity and higher W^+W^- cross section. For intermediate ΔM values different from those chosen for optimisation we choose the combination of selections (low, medium and high ΔM) providing the highest sensitivity [6]. In this combination procedure, we take into account the overlap among the selections within the data and Monte Carlo samples.

A summary of the searches at 183 GeV is given in Table 1. It should be noted that the same event can be selected by more than one selection. No excess of events is observed relative to the expected Standard Model background.

Selection	Low ΔM		Medium ΔM		High ΔM		Combined	
	N_{data}	N_{exp}	N_{data}	N_{exp}	N_{data}	N_{exp}	N_{data}	N_{exp}
$\tilde{e}^{\pm}$	1	1.1 ± 0.6	1	2.8 ± 0.8	2	3.8 ± 0.3	3	6.9 ± 1.1
$\tilde{\mu}^{\pm}$	1	3.2 ± 1.5	1	3.0 ± 1.3	4	3.0 ± 0.3	4	6.1 ± 1.5
$\tilde{\tau}^{\pm}$	2	1.5 ± 0.5	2	4.1 ± 0.6	11	10.0 ± 0.6	13	11.6 ± 0.7
Combined	4	5.7 ± 1.7	4	9.2 ± 1.6	16	15.5 ± 0.7	19	22.7 ± 1.9

Table 1: Number of observed events, N_{data}, and expected events from Standard Model processes, N_{exp}, for each selection separately and for combinations of them. The error on the Monte Carlo prediction is mainly due to the limited statistics for two-photon interactions.

Figure 3 shows the efficiencies for scalar leptons as a function of ΔM. The efficiencies for the low, medium and high ΔM selections are shown separately. The efficiency of the combined selection, in the mass region close to the expected limit, reaches 68% for scalar electrons (Figure 3a), 46% for scalar muons (Figure 3b), and 31% for scalar taus (Figure 3c).

5 Model independent limits on production cross sections

5.1 Stable scalar leptons

No signal events are recorded in any of the data samples for the three sets of selection requirements. This is converted into an upper limit on the production cross section of stable scalar leptons at 183 GeV. The relative systematic error, which is mainly due to limited Monte Carlo statistics, is estimated to be 5% and is taken into account by reducing the selection efficiency by one standard deviation. The luminosity for the data at lower centre-of-mass energies is scaled to 183 GeV according to the ratio $\sigma(E_{\sqrt{s}})/\sigma(183)$, where σ is the cross section for a given scalar lepton mass.

Figure 4 shows the upper limit on the cross section at 183 GeV as a function of the scalar lepton mass. The upper limit on the production cross section for pair production of long-lived scalar leptons, in the mass range $50 - 90$ GeV, is below $0.06 - 0.10$ pb and below 0.2 pb in the mass range $45 - 50$ GeV. Also shown in Figure 4 is the predicted SUSY cross section for the scalar partners of the left- and right-handed muons or taus as a function of mass at 183 GeV. In the MSSM, we exclude long-lived scalar leptons with a mass smaller than 81.2 GeV ($\tilde{\ell}^{\pm}_R$) and 82.2 GeV ($\tilde{\ell}^{\pm}_L$), at 95% C.L.

5.2 Unstable scalar leptons

We set upper limits on scalar lepton production cross sections. These limits, at 95% C.L., are derived taking into account background contributions. As the background from two-photon interactions is not well described by the Monte Carlo, in the evaluation of the limits, we conservatively assume no contribution from this source. Systematic errors on the signal efficiency, dominated by Monte Carlo statistics, are smaller than 5%. These errors are taken into account following the procedure explained in Reference 20.

To derive upper limits on production cross sections, we combine data collected at 183 GeV with those collected from 130 to 172 GeV [6, 8]. The combination is performed without any scaling of the cross section. Hence these limits should be interpreted as limits on the luminosity-weighted average cross section ($\mathcal{L}_{\mathrm{TOT}}^{-1} \sum_{\mathrm{E}_{\sqrt{s}}} \sigma(\mathrm{E}_{\sqrt{s}}) \mathcal{L}(\mathrm{E}_{\sqrt{s}})$).

Figure 5 shows the upper limits set on the production cross section of scalar electrons, scalar muons and scalar taus, in the plane $M_{\tilde{\chi}_1^0} - M_{\tilde{\ell}^\pm}$. These upper limits are derived under the assumption of a 100% branching fraction $\tilde{\ell}^\pm \rightarrow \tilde{\chi}_1^0 \ell^\pm$. The upper limit for scalar electrons takes into account the decrease of the selection efficiency, which occurs when scalar electrons are produced via the t-channel, which is dominant for light neutralinos. For scalar electrons and muons with medium ΔM, cross sections larger than 0.15 pb are excluded. Owing to the lower selection efficiency, the corresponding upper limit for the scalar tau cross section is 0.3 pb.

6 Limits on unstable scalar leptons in the MSSM

To derive limits in the MSSM, we optimise the combination of selections for each point on a fine grid in the MSSM parameter space. At each point the combination of selections providing the highest sensitivity, given the production cross sections and the decay branching fractions, is chosen.

In the MSSM, with Grand Unification assumption [21], the masses and couplings of the supersymmetric particles as well as their production cross sections, are entirely described once five parameters are fixed: the ratio of the vacuum expectation values of the two Higgs doublets, $\tan\beta$, the gaugino mass parameter, M_2, the higgsino mixing parameter, μ, the common mass for scalar fermions at the GUT scale, m_0, and the trilinear coupling in the Higgs sector, A. We investigate the following region in the MSSM parameter space:

$$\begin{array}{rcl@{\qquad}rcl} 1 \leq & \tan\beta & \leq 40, & 0 \leq & M_2 & \leq 2000 \text{ GeV}, \\ -500 \text{ GeV} \leq & \mu & \leq 500 \text{ GeV}, & 10 \text{ GeV} \leq & m_0 & \leq 500 \text{ GeV}. \end{array}$$

The interpretation in the MSSM of the search results presented here do not depend on the value of A except for the exclusion of scalar taus.

All cross section limits previously shown can be translated into excluded regions of the MSSM parameter space. To derive such exclusions, experimental results are confronted to theoretical cross sections and branching fractions as computed with the program `SUSYGEN`.

In general, the SUSY partners of the right-handed leptons ($\tilde{\ell}_R^\pm$) are expected to be lighter than their counterparts for left-handed leptons. Hence, we show in Figures 6a, 6b and 6c the exclusion contours in the $M_{\tilde{\chi}_1^0} - M_{\tilde{\ell}_R^\pm}$ plane considering only the reaction $\mathrm{e^+e^-} \rightarrow \tilde{\ell}_R^\pm \tilde{\ell}_R^\mp$ and setting $\mu = -200$ GeV and $\tan\beta = \sqrt{2}$. These exclusions hold also for higher $\tan\beta$ and $|\mu|$ values. For smaller $|\mu|$ values, the t-channel contribution to the scalar electron cross section is reduced, thus reducing by a few GeV the limit on its mass shown in Figure 6a. The values of μ and $\tan\beta$ are also relevant for the calculation of the branching ratio for the decay $\tilde{\ell}^{\pm} \to \tilde{\chi}^0_2\ell^{\pm} \to \tilde{\chi}^0_1 Z^* \ell^{\pm}$ in Figures 6a–c. To derive these exclusions, only the purely leptonic decay $\tilde{\ell}^{\pm}_R \to \ell^{\pm}\tilde{\chi}^0_1$ is considered, neglecting any additional efficiency from cascade decays.

Under these assumptions lower limits on scalar lepton masses are derived. From Figures 6a and 6b scalar electrons lighter than 80GeV, for $\Delta M > 20$ GeV, and scalar muons lighter than 66 GeV, for $\Delta M > 6$ GeV, are excluded. From Figure 6c we conclude that scalar taus lighter than 53 GeV, for $\Delta M > 10$ GeV, are excluded if there is no mixing.

Mass eigenstates of scalar leptons are in general a mixture of the weak eigenstates $\tilde{\ell}^{\pm}_R$ and $\tilde{\ell}^{\pm}_L$. The mixing between $\tilde{\ell}^{\pm}_R$ and $\tilde{\ell}^{\pm}_L$ is proportional to the mass of the partner lepton. Hence the mixing for scalar electrons and muons is always negligible while it can be sizable for scalar taus. The mixing is governed by the parameters A, μ and $\tan\beta$.

Scalar tau mass eigenstates are given by $\tilde{\tau}_{1,2} = \tilde{\tau}_{L,R}\cos\theta_{\rm LR} \pm \tilde{\tau}_{R,L}\sin\theta_{\rm LR}$, where $\theta_{\rm LR}$ is the mixing angle. The production cross section for scalar taus can be parametrised as a function of the scalar tau mass and of the mixing angle [22]. At $\theta_{\rm LR} \sim 0.52^{\circ}$ the scalar tau decouples from the Z and the cross section is minimal. It reaches the maximum at $\cos\theta_{\rm LR}$=1 when the scalar tau is equivalent to the weak eigenstate $\tilde{\tau}^{\pm}_L$.

The exclusion contours in Figure 6d are obtained considering only the reaction $e^+e^- \to \tilde{\tau}^+_1\,\tilde{\tau}^-_1$ and using the same values as above for μ and $\tan\beta$ for the calculation of the rate of cascade decays, for which we neglect any additional efficiency. The two contours correspond to the minimal and maximal cross sections. Even under the most conservative assumption for the mixing the above mass limits for scalar taus hold. The differences between the experimental and average limits in Figures 6c and 6d do not reflect a disagreement between data and Monte Carlo (see Table 1) but merely that the cross section is relatively insensitive to the mass far from the kinematic limit.

Mass limits on scalar electrons and muons can also be expressed in terms of the M_2 and m_0 parameters. This is shown in Figure 7 where exclusion domains in the $M_2 - m_0$ plane are presented for several $\tan\beta$ values and for $\mu = -200$ GeV. The exclusions in Figure 7 are obtained by combining scalar electron and muon searches with chargino and neutralino searches [23]. The two contributions are well separated, as the contribution from scalar lepton searches is dominant for $m_0 \lesssim 70$ GeV while that from chargino and neutralino is dominant for $m_0 \gtrsim 70$ GeV. In Figure 7 is also shown for comparison the exclusion obtained by D0, at Tevatron, from a search for gluinos and scalar quarks [24]. The exclusion by D0 is determined in the minimal supergravity framework [2], which is equivalent to that adopted in this paper if large values for $|\mu|$ are taken, such as $\mu = -200$ GeV.

In summary, improved limits on scalar leptons are presented. Long-lived scalar leptons lighter than 81.2 GeV ($\tilde{\ell}^{\pm}_R$) and 82.2 GeV ($\tilde{\ell}^{\pm}_L$) are excluded at 95% C.L. Unstable scalar electrons lighter than 80 GeV, for $\Delta M > 20$ GeV, and scalar muons lighter than 66 GeV, for $\Delta M >$ 6 GeV, are excluded for most of the possible values for the MSSM parameters. Unstable scalar taus lighter than 53 GeV, for $\Delta M > 10$ GeV, are excluded under the most conservative assumption for the mixing.

Acknowledgements

We wish to express our gratitude to the CERN accelerator divisions for the excellent performance of the LEP machine. We acknowledge the efforts of the engineers and technicians who have participated in the construction and maintenance of this experiment.

References

[1] Y.A. Golfand and E.P. Likhtman, Sov. Phys. JETP **13** (1971) 323;
D.V. Volkhov and V.P. Akulov, Phys. Lett. **B 46** (1973) 109;
J. Wess and B. Zumino, Nucl. Phys. **B 70** (1974) 39;
P. Fayet and S. Ferrara, Phys. Rep. **C 32** (1977) 249;
A. Salam and J. Strathdee, Fortschr. Phys. **26** (1978) 57.

[2] H. P. Nilles, Phys. Rep. **110** (1984) 1;
H. E. Haber and G. L. Kane, Phys. Rep. **117** (1985) 75;
R. Barbieri, Nuovo Cimento **11** No. 4 (1988) 1.

[3] See for instance:
C. Kolda, Nucl. Phys. Proc. Suppl. **62** (1998) 266.

[4] L.J. Hall and M. Suzuki, Nucl. Phys. **B 231** (1984) 419;
D.E. Brahm and L.J. Hall, Phys. Rev. **D 40** (1989) 2449;
L. Ibanez and G. Ross, Nucl. Phys. **B 368** (1992) 3;
A. Chamseddine and H. Dreiner, Nucl. Phys. **B 458** (1996) 65;
A.Y. Smirnov and F. Vissani, Nucl. Phys. **B 460** (1996) 37.

[5] S. Dimopoulos *et al.*, Nucl. Phys. **B 488** (1997) 39;
S. Ambrosanio *et al.*, Phys. Rev. **D 56** (1997) 1761;
G.F. Giudice and R. Rattazzi, CERN-TH-97-380, (1997), hep-ph/9801271.

[6] L3 Collab., M. Acciarri *et al.*, Eur. Phys. Journal **C 4** (1998) 207.

[7] ALEPH Collab., R. Barate *et al.*, Phys. Lett. **B 433** (1998) 176;
DELPHI Collab., P. Abreu *et al.*, CERN-EP-98-116, (1998);
OPAL Collab., G. Abbiendi *et al.*, CERN-EP-98-122, (1998).

[8] L3 Collab., O. Adriani *et al.*, Phys. Rep. **236** (1993) 1;
L3 Collab., M. Acciarri *et al.*, Phys. Lett. **B 350** (1995) 109;
L3 Collab., M. Acciarri *et al.*, Phys. Lett. **B 377** (1996) 289.

[9] L3 Collab., B. Adeva *et al.*, Nucl. Instr. and Meth. **A 289** (1990) 35;
M. Chemarin *et al.*, Nucl. Instr. and Meth. **A 349** (1994) 345;
M. Acciarri *et al.*, Nucl. Instr. and Meth. **A 351** (1994) 300;
G. Basti *et al.*, Nucl. Instr. and Meth. **A 374** (1996) 293;
I.C. Brock *et al.*, Nucl. Instr. and Meth. **A 381** (1996) 236;
A. Adam *et al.*, Nucl. Instr. and Meth. **A 383** (1996) 342.

[10] T. Sjöstrand, "PYTHIA 5.7 and JETSET 7.4 Physics and Manual",
CERN–TH/7112/93 (1993), revised August 1995;
T. Sjöstrand, Comp. Phys. Comm. **82** (1994) 74.

[11] F.A. Berends, R. Kleiss and R. Pittau, Nucl. Phys. **B 424** (1994) 308; Nucl. Phys. **B 426** (1994) 344; Nucl. Phys. (Proc. Suppl.) **B 37** (1994) 163; Phys. Lett. **B 335** (1994) 490; Comp. Phys. Comm. **83** (1994) 141.

[12] The `KORALZ` version 4.02 is used.
S. Jadach, B.F.L. Ward and Z. Wąs, Comp. Phys. Comm. **79** (1994) 503.

[13] J.H. Field, Phys. Lett. **B 323** (1994) 432;
J.H. Field and T. Riemann, Comp. Phys. Comm. **94** (1996) 53.

[14] `KORALW` version 1.33 is used.
M. Skrzypek *et al.*, Comp. Phys. Comm. **94** (1996) 216;
M. Skrzypek *et al.*, Phys. Lett. **B 372** (1996) 289.

[15] F.A. Berends, P.H. Daverfeldt and R. Kleiss, Nucl. Phys. **B 253** (1985) 441.

[16] `PHOJET` version 1.10 is used.
R. Engel, Z. Phys. **C 66** (1995) 203;
R. Engel and J. Ranft, Phys. Rev. **D 54** (1996) 4244.

[17] `SUSYGEN` version 2.2 is used.
S. Katsanevas and P. Morawitz, Comp. Phys. Comm. **112** (1998) 227.

[18] The L3 detector simulation is based on GEANT Version 3.15.
See R. Brun *et al.*, "GEANT 3", CERN DD/EE/84-1 (Revised), September 1987.

[19] H. Fesefeldt, RWTH Aachen Preprint PITHA 85/02 (1985).

[20] R.D. Cousins and V.L. Highland, Nucl. Inst. Meth. **A 320** (1992) 331.

[21] See for instance:
L. Ibanez, Phys. Lett. **B 118** (1982) 73;
R. Barbieri, S. Farrara and C. Savoy, Phys. Lett. **B 119** (1982) 343.

[22] A. Bartl *et al.*, Z. Phys. **C 73** (1997) 469.

[23] The L3 Collaboration, Search for Charginos and Neutralinos in e^+e^- Collissions at $\sqrt{s} = 161 - 183$ GeV, contributed paper n. 493 to the *ICHEP98, Vancouver, B.C., Canada, July 1998*; paper in preparation.

[24] D0 Collab., S. Abachi *et al.*, Proceedings of the 28^{th} ICHEP, Warsaw, (1996);
D0 Collab., B. Abbott *et al.*, Proceedings of the XVIII Int. Symposium on Lepton Photon Interactions, Hamburg, (1997).

The L3 Collaboration:

M.Acciarri,[26] P.Achard,[18] O.Adriani,[15] M.Aguilar-Benitez,[25] J.Alcaraz,[25] G.Alemanni,[21] J.Allaby,[16] A.Aloisio,[28] M.G.Alviggi,[28] G.Ambrosi,[18] H.Anderhub,[47] V.P.Andreev,[6,36] T.Angelescu,[12] F.Anselmo,[9] A.Arefiev,[27] T.Azemoon,[3] T.Aziz,[10] P.Bagnaia,[35] L.Baksay,[42] A.Balandras,[4] R.C.Ball,[3] S.Banerjee,[10] Sw.Banerjee,[10] K.Banicz,[44] A.Barczyk,[47,45] R.Barillère,[16] L.Barone,[35] P.Bartalini,[21] M.Basile,[9] R.Battiston,[32] A.Bay,[21] F.Becattini,[15] U.Becker,[14] F.Behner,[47] J.Berdugo,[25] P.Berges,[14] B.Bertucci,[32] B.L.Betev,[47] S.Bhattacharya,[10] M.Biasini,[32] A.Biland,[47] J.J.Blaising,[4] S.C.Blyth,[33] G.J.Bobbink,[2] A.Böhm,[1] L.Boldizsar,[13] B.Borgia,[16,35] D.Bourilkov,[47] M.Bourquin,[18] S.Braccini,[18] J.G.Branson,[38] V.Brigljevic,[47] F.Brochu,[4] A.Buffini,[15] A.Buijs,[43] J.D.Burger,[14] W.J.Burger,[32] J.Busenitz,[42] A.Button,[3] X.D.Cai,[14] M.Campanelli,[47] M.Capell,[14] G.Cara Romeo,[9] G.Carlino,[28] A.M.Cartacci,[15] J.Casaus,[25] G.Castellini,[15] F.Cavallari,[35] N.Cavallo,[28] C.Cecchi,[18] M.Cerrada,[25] F.Cesaroni,[22] M.Chamizo,[18] Y.H.Chang,[49] U.K.Chaturvedi,[17] M.Chemarin,[24] A.Chen,[49] G.Chen,[7] G.M.Chen,[7] H.F.Chen,[19] H.S.Chen,[7] X.Chereau,[4] G.Chiefari,[28] L.Cifarelli,[37] F.Cindolo,[9] C.Civinini,[15] I.Clare,[14] R.Clare,[14] G.Coignet,[4] A.P.Colijn,[2] N.Colino,[25] S.Costantini,[8] F.Cotorobai,[12] B.Cozzoni,[9] B.de la Cruz,[25] A.Csilling,[13] T.S.Dai,[14] J.A.van Dalen,[30] R.D'Alessandro,[15] R.de Asmundis,[28] P.Deglon,[18] A.Degré,[4] K.Deiters,[45] D.della Volpe,[28] P.Denes,[34] F.DeNotaristefani,[35] A.De Salvo,[47] M.Diemoz,[35] D.van Dierendonck,[2] F.Di Lodovico,[47] C.Dionisi,[16,35] M.Dittmar,[47] A.Dominguez,[38] A.Doria,[28] M.T.Dova,[17,♯] D.Duchesneau,[4] D.Dufournand,[4] P.Duinker,[2] I.Duran,[39] H.El Mamouni,[24] A.Engler,[33] F.J.Eppling,[14] F.C.Erné,[2] P.Extermann,[18] M.Fabre,[45] R.Faccini,[35] M.A.Falagan,[25] S.Falciano,[35] A.Favara,[15] J.Fay,[24] O.Fedin,[36] M.Felcini,[47] T.Ferguson,[33] F.Ferroni,[35] H.Fesefeldt,[1] E.Fiandrini,[32] J.H.Field,[18] F.Filthaut,[16] P.H.Fisher,[14] I.Fisk,[38] G.Forconi,[14] L.Fredj,[18] K.Freudenreich,[47] C.Furetta,[26] Yu.Galaktionov,[27,14] S.N.Ganguli,[10] P.Garcia-Abia,[5] M.Gataullin,[31] S.S.Gau,[11] S.Gentile,[35] N.Gheordanescu,[12] S.Giagu,[35] Z.F.Gong,[19] G.Grenier,[24] M.W.Gruenewald,[8] R.van Gulik,[2] V.K.Gupta,[34] A.Gurtu,[10] L.J.Gutay,[44] D.Haas,[5] A.Hasan,[29] D.Hatzifotiadou,[9] T.Hebbeker,[8] A.Hervé,[16] P.Hidas,[13] J.Hirschfelder,[33] H.Hofer,[47] G. Holzner,[47] H.Hoorani,[33] S.R.Hou,[49] I.Iashvili,[46] B.N.Jin,[7] L.W.Jones,[3] P.de Jong,[2] I.Josa-Mutuberría,[25] R.A.Khan,[17] D.Kamrad,[46] J.S.Kapustinsky,[23] M.Kaur,[17,♢] M.N.Kienzle-Focacci,[18] D.Kim,[35] D.H.Kim,[41] J.K.Kim,[41] S.C.Kim,[41] W.W.Kinnison,[23] J.Kirkby,[16] D.Kiss,[13] W.Kittel,[30] A.Klimentov,[14,27] A.C.König,[30] A.Kopp,[46] I.Korolko,[27] V.Koutsenko,[14,27] R.W.Kraemer,[33] W.Krenz,[1] A.Kunin,[14,27] P.Lacentre,[46,♮,♯] P.Ladron de Guevara,[25] I.Laktineh,[24] G.Landi,[15] K.Lassila-Perini,[47] P.Laurikainen,[20] A.Lavorato,[37] M.Lebeau,[16] A.Lebedev,[14] P.Lebrun,[24] P.Lecomte,[47] P.Lecoq,[16] P.Le Coultre,[47] H.J.Lee,[8] J.M.Le Goff,[16] R.Leiste,[46] E.Leonardi,[35] P.Levtchenko,[36] C.Li,[19] C.H.Lin,[49] W.T.Lin,[49] F.L.Linde,[2,16] L.Lista,[28] Z.A.Liu,[7] W.Lohmann,[46] E.Longo,[35] Y.S.Lu,[7] K.Lübelsmeyer,[1] C.Luci,[16,35] D.Luckey,[14] L.Lugnier,[24] L.Luminari,[35] W.Lustermann,[47] W.G.Ma,[19] M.Maity,[10] G.Majumder,[10] L.Malgeri,[16] A.Malinin,[27] C.Maña,[25] D.Mangeol,[30] P.Marchesini,[47] G.Marian,[42,¶] J.P.Martin,[24] F.Marzano,[35] G.G.G.Massaro,[2] K.Mazumdar,[10] R.R.McNeil,[6] S.Mele,[16] L.Merola,[28] M.Meschini,[15] W.J.Metzger,[30] M.von der Mey,[1] D.Migani,[9] A.Mihul,[12] H.Milcent,[16] G.Mirabelli,[35] J.Mnich,[16] P.Molnar,[8] B.Monteleoni,[15] T.Moulik,[10] G.S.Muanza,[24] F.Muheim,[18] A.J.M.Muijs,[2] M.Napolitano,[28] F.Nessi-Tedaldi,[47] H.Newman,[31] T.Niessen,[1] A.Nisati,[35] H.Nowak,[46] Y.D.Oh,[41] G.Organtini,[35] R.Ostonen,[20] C.Palomares,[25] D.Pandoulas,[1] S.Paoletti,[35,16] P.Paolucci,[28] H.K.Park,[33] I.H.Park,[41] G.Pascale,[35] G.Passaleva,[16] S.Patricelli,[28] T.Paul,[11] M.Pauluzzi,[32] C.Paus,[16] F.Pauss,[47] D.Peach,[16] M.Pedace,[35] Y.J.Pei,[1] S.Pensotti,[26] D.Perret-Gallix,[4] B.Petersen,[30] S.Petrak,[8] D.Piccolo,[28] M.Pieri,[15] P.A.Piroué,[34] E.Pistolesi,[26] V.Plyaskin,[27] M.Pohl,[47] V.Pojidaev,[27,15] H.Postema,[14] J.Pothier,[16] N.Produit,[18] D.Prokofiev,[36] J.Quartieri,[37] G.Rahal-Callot,[47] N.Raja,[10] P.G.Rancoita,[26] G.Raven,[38] P.Razis,[29] D.Ren,[47] M.Rescigno,[35] S.Reucroft,[11] T.van Rhee,[43] S.Riemann,[46] K.Riles,[3] A.Robohm,[47] J.Rodin,[42] B.P.Roe,[3] L.Romero,[25] S.Rosier-Lees,[4] J.A.Rubio,[16] D.Ruschmeier,[8] H.Rykaczewski,[47] S.Sakar,[35] J.Salicio,[16] E.Sanchez,[16] M.P.Sanders,[30] M.E.Sarakinos,[20] C.Schäfer,[1] V.Schegelsky,[36] S.Schmidt-Kaerst,[1] D.Schmitz,[1] N.Scholz,[47] H.Schopper,[48] D.J.Schotanus,[30] J.Schwenke,[1] G.Schwering,[1] C.Sciacca,[28] D.Sciarrino,[18] A.Seganti,[9] L.Servoli,[32] S.Shevchenko,[31] N.Shivarov,[40] V.Shoutko,[27] J.Shukla,[23] E.Shumilov,[27] A.Shvorob,[31] T.Siedenburg,[1] D.Son,[41] B.Smith,[33] P.Spillantini,[15] M.Steuer,[14] D.P.Stickland,[34] A.Stone,[6] H.Stone,[34] B.Stoyanov,[40] A.Straessner,[1] K.Sudhakar,[10] G.Sultanov,[17] L.Z.Sun,[19] H.Suter,[47] J.D.Swain,[17] Z.Szillasi,[42,¶] X.W.Tang,[7] L.Tauscher,[5] L.Taylor,[11] C.Timmermans,[30] Samuel C.C.Ting,[14] S.M.Ting,[14] S.C.Tonwar,[10] J.Tóth,[13] C.Tully,[34] K.L.Tung,[7] Y.Uchida,[14] J.Ulbricht,[47] E.Valente,[35] G.Vesztergombi,[13] I.Vetlitsky,[27] D.Vicinanza,[37] G.Viertel,[47] S.Villa,[11] M.Vivargent,[4] S.Vlachos,[5] I.Vodopianov,[36] H.Vogel,[33] H.Vogt,[46] I.Vorobiev,[16,27] A.A.Vorobyov,[36] A.Vorvolakos,[29] M.Wadhwa,[5] W.Wallraff,[1] M.Wang,[14] X.L.Wang,[19] Z.M.Wang,[19] A.Weber,[1] M.Weber,[1] P.Wienemann,[1] H.Wilkens,[30] S.X.Wu,[14] S.Wynhoff,[1] L.Xia,[31] Z.Z.Xu,[19] B.Z.Yang,[19] C.G.Yang,[7] H.J.Yang,[7] M.Yang,[7] J.B.Ye,[19] S.C.Yeh,[50] J.M.You,[33] An.Zalite,[36] Yu.Zalite,[36] P.Zemp,[47] Z.P.Zhang,[19] G.Y.Zhu,[7] R.Y.Zhu,[31] A.Zichichi,[9,16,17] F.Ziegler,[46] G.Zilizi,[42,¶] M.Zöller.[1]

1 I. Physikalisches Institut, RWTH, D-52056 Aachen, FRG[§]
III. Physikalisches Institut, RWTH, D-52056 Aachen, FRG[§]
2 National Institute for High Energy Physics, NIKHEF, and University of Amsterdam, NL-1009 DB Amsterdam, The Netherlands
3 University of Michigan, Ann Arbor, MI 48109, USA
4 Laboratoire d'Annecy-le-Vieux de Physique des Particules, LAPP,IN2P3-CNRS, BP 110, F-74941 Annecy-le-Vieux CEDEX, France
5 Institute of Physics, University of Basel, CH-4056 Basel, Switzerland
6 Louisiana State University, Baton Rouge, LA 70803, USA
7 Institute of High Energy Physics, IHEP, 100039 Beijing, China[△]
8 Humboldt University, D-10099 Berlin, FRG[§]
9 University of Bologna and INFN-Sezione di Bologna, I-40126 Bologna, Italy
10 Tata Institute of Fundamental Research, Bombay 400 005, India
11 Northeastern University, Boston, MA 02115, USA
12 Institute of Atomic Physics and University of Bucharest, R-76900 Bucharest, Romania
13 Central Research Institute for Physics of the Hungarian Academy of Sciences, H-1525 Budapest 114, Hungary[‡]
14 Massachusetts Institute of Technology, Cambridge, MA 02139, USA
15 INFN Sezione di Firenze and University of Florence, I-50125 Florence, Italy
16 European Laboratory for Particle Physics, CERN, CH-1211 Geneva 23, Switzerland
17 World Laboratory, FBLJA Project, CH-1211 Geneva 23, Switzerland
18 University of Geneva, CH-1211 Geneva 4, Switzerland
19 Chinese University of Science and Technology, USTC, Hefei, Anhui 230 029, China[△]
20 SEFT, Research Institute for High Energy Physics, P.O. Box 9, SF-00014 Helsinki, Finland
21 University of Lausanne, CH-1015 Lausanne, Switzerland
22 INFN-Sezione di Lecce and Universitá Degli Studi di Lecce, I-73100 Lecce, Italy
23 Los Alamos National Laboratory, Los Alamos, NM 87544, USA
24 Institut de Physique Nucléaire de Lyon, IN2P3-CNRS,Université Claude Bernard, F-69622 Villeurbanne, France
25 Centro de Investigaciones Energéticas, Medioambientales y Tecnologícas, CIEMAT, E-28040 Madrid, Spain♭
26 INFN-Sezione di Milano, I-20133 Milan, Italy
27 Institute of Theoretical and Experimental Physics, ITEP, Moscow, Russia
28 INFN-Sezione di Napoli and University of Naples, I-80125 Naples, Italy
29 Department of Natural Sciences, University of Cyprus, Nicosia, Cyprus
30 University of Nijmegen and NIKHEF, NL-6525 ED Nijmegen, The Netherlands
31 California Institute of Technology, Pasadena, CA 91125, USA
32 INFN-Sezione di Perugia and Universitá Degli Studi di Perugia, I-06100 Perugia, Italy
33 Carnegie Mellon University, Pittsburgh, PA 15213, USA
34 Princeton University, Princeton, NJ 08544, USA
35 INFN-Sezione di Roma and University of Rome, "La Sapienza", I-00185 Rome, Italy
36 Nuclear Physics Institute, St. Petersburg, Russia
37 University and INFN, Salerno, I-84100 Salerno, Italy
38 University of California, San Diego, CA 92093, USA
39 Dept. de Fisica de Particulas Elementales, Univ. de Santiago, E-15706 Santiago de Compostela, Spain
40 Bulgarian Academy of Sciences, Central Lab. of Mechatronics and Instrumentation, BU-1113 Sofia, Bulgaria
41 Center for High Energy Physics, Adv. Inst. of Sciences and Technology, 305-701 Taejon, Republic of Korea
42 University of Alabama, Tuscaloosa, AL 35486, USA
43 Utrecht University and NIKHEF, NL-3584 CB Utrecht, The Netherlands
44 Purdue University, West Lafayette, IN 47907, USA
45 Paul Scherrer Institut, PSI, CH-5232 Villigen, Switzerland
46 DESY-Institut für Hochenergiephysik, D-15738 Zeuthen, FRG
47 Eidgenössische Technische Hochschule, ETH Zürich, CH-8093 Zürich, Switzerland
48 University of Hamburg, D-22761 Hamburg, FRG
49 National Central University, Chung-Li, Taiwan, China
50 Department of Physics, National Tsing Hua University, Taiwan, China
§ Supported by the German Bundesministerium für Bildung, Wissenschaft, Forschung und Technologie
‡ Supported by the Hungarian OTKA fund under contract numbers T019181, F023259 and T024011.
¶ Also supported by the Hungarian OTKA fund under contract numbers T22238 and T026178.
♭ Supported also by the Comisión Interministerial de Ciencia y Tecnología.
♯ Also supported by CONICET and Universidad Nacional de La Plata, CC 67, 1900 La Plata, Argentina.
♮ Supported by Deutscher Akademischer Austauschdienst.
◇ Also supported by Panjab University, Chandigarh-160014, India.
△ Supported by the National Natural Science Foundation of China.

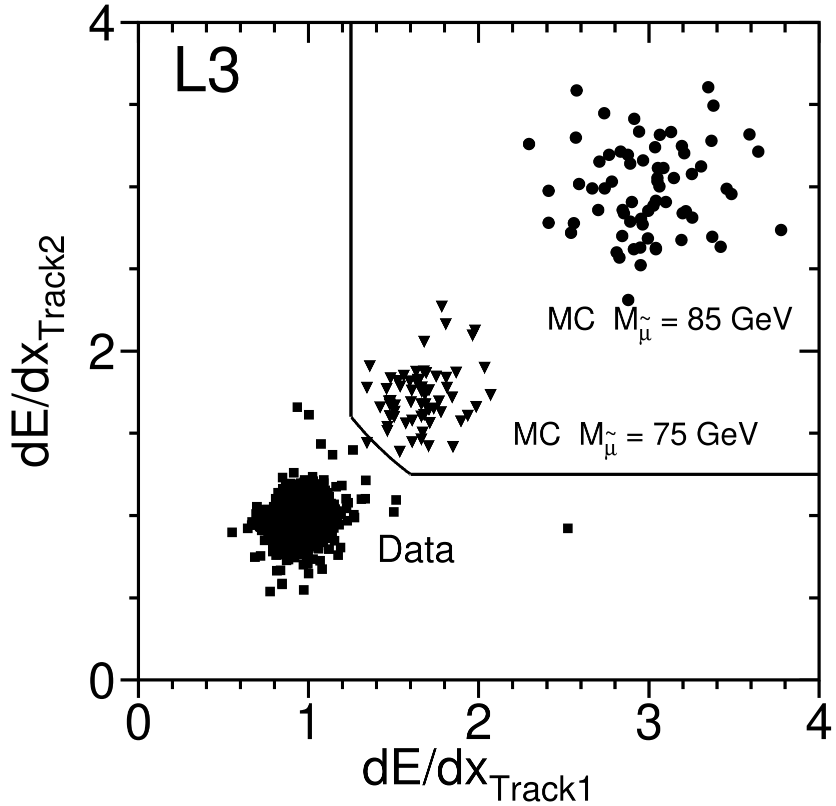

Figure 1: The measured ionization energy loss of track 2 versus track 1, for the highest energy data, at 183 GeV, and the simulated signal for stable scalar leptons with masses of 75 GeV and 85 GeV. The lines represent the selection requirements.

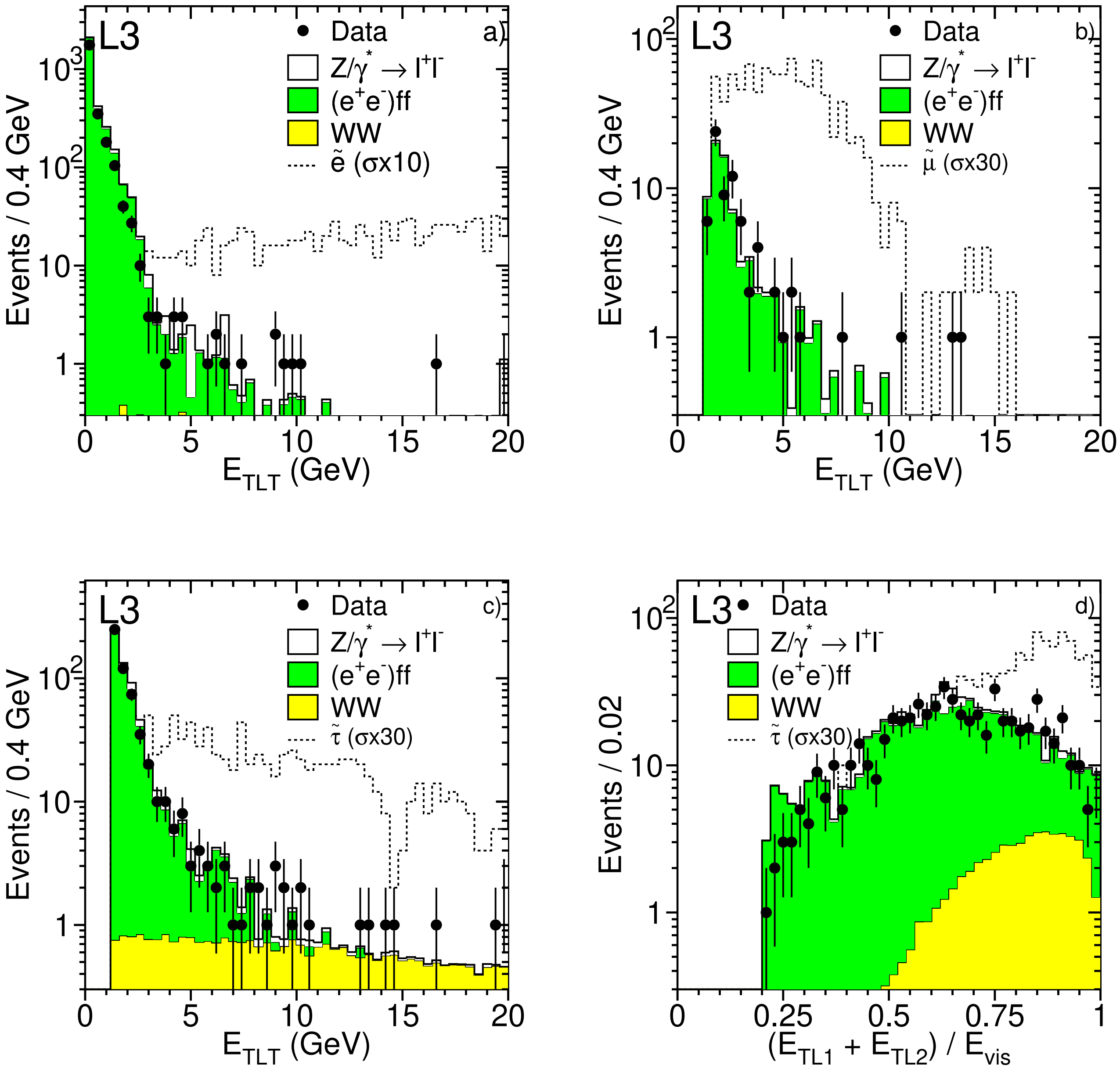

Figure 2: Distributions at the preselection level for the most important variables of scalar lepton selections. Data at 183 GeV are compared to Standard Model background processes (solid line) and to the expected signal (dashed line): a) the variable E_{TLT} (see section 4) in the scalar electron selection, b) the variable E_{TLT} in the scalar muon selection, c) the variable E_{TLT} and d) the normalised sum of taus transverse energies (E_{TL}) in the scalar tau selection. The signal distributions are evaluated a) for $M_{\tilde{e}} = 60$ GeV and $\Delta M = 45$ GeV, b) for $M_{\tilde{\mu}} = 60$ GeV and $\Delta M = 5$ GeV, c) and d) for $M_{\tilde{\tau}} = 55$ GeV and $M_{\tilde{\chi}_1^0} = 25$ GeV.

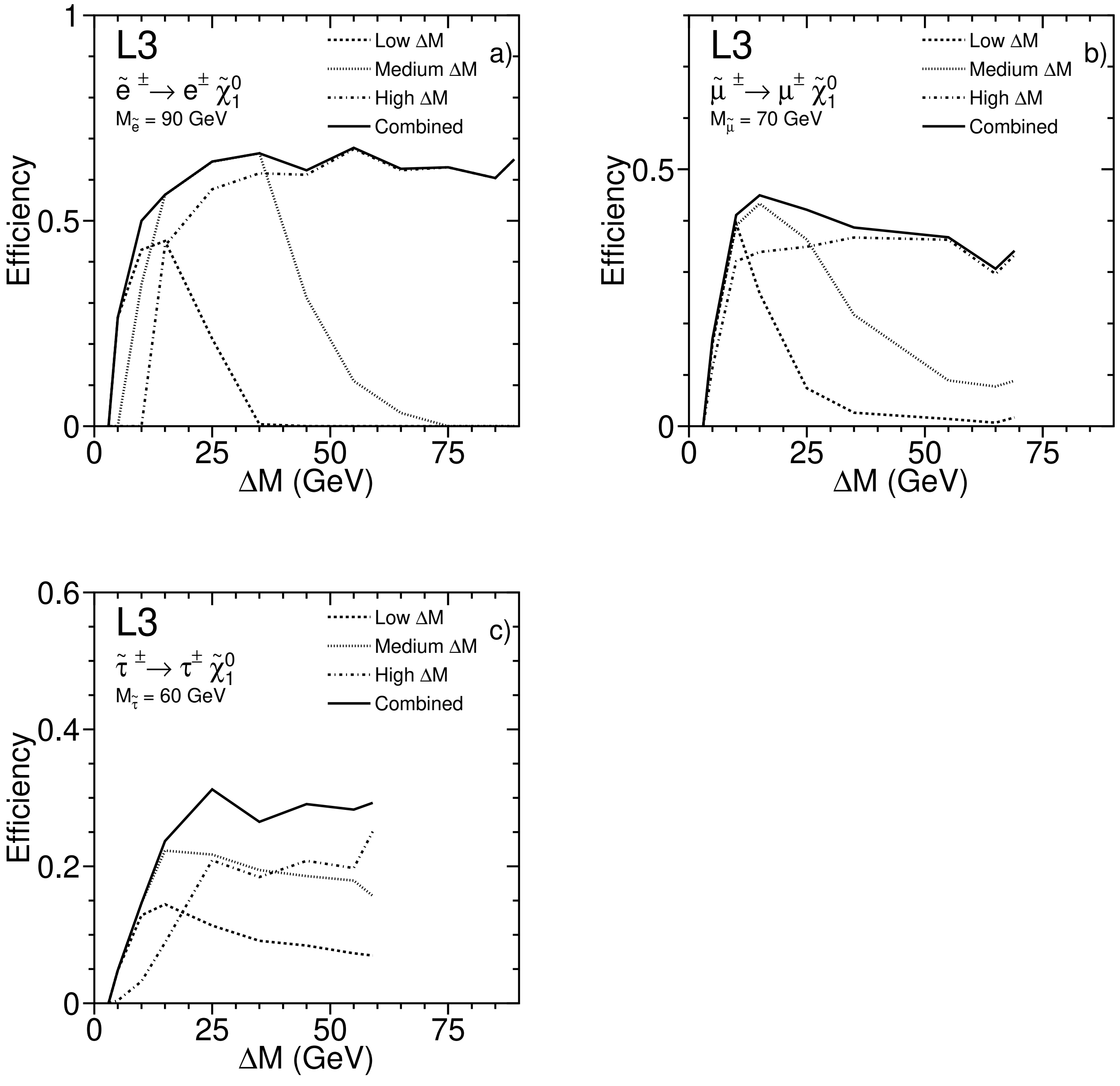

Figure 3: Efficiencies as a function of ΔM for scalar leptons: a) scalar electrons ($M_{\tilde{e}} = 90$ GeV), b) scalar muons ($M_{\tilde{\mu}} = 70$ GeV) and c) scalar taus ($M_{\tilde{\tau}} = 60$ GeV). The efficiencies for the low, medium and high ΔM selections as well as for the combined selection are shown. These efficiencies are given for the decay $\tilde{\ell}^{\pm} \rightarrow \ell^{\pm}\tilde{\chi}^0_1$.

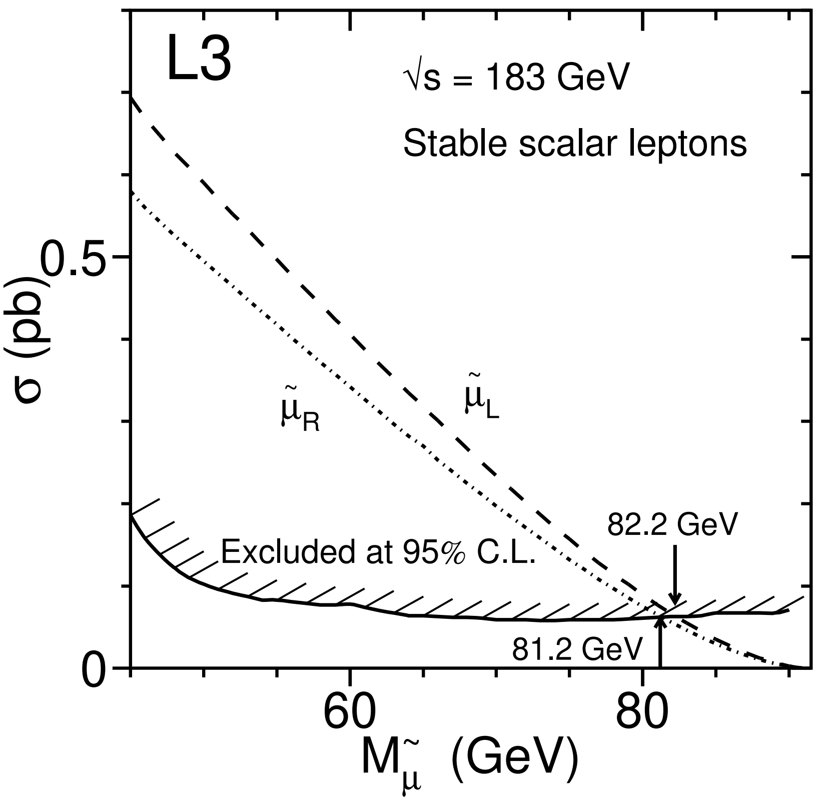

Figure 4: Model independent upper limit on the production cross section for pair-production of stable scalar leptons at 183 GeV. The theoretical predictions for the pair-production cross sections of $\tilde{\mu}_R$ and $\tilde{\mu}_L$ are also shown. Lower mass limits for long-lived scalar leptons of 81.2 GeV ($\tilde{\ell}^{\pm}_R$) and 82.2 GeV ($\tilde{\ell}^{\pm}_L$) are obtained as indicated by the arrows.

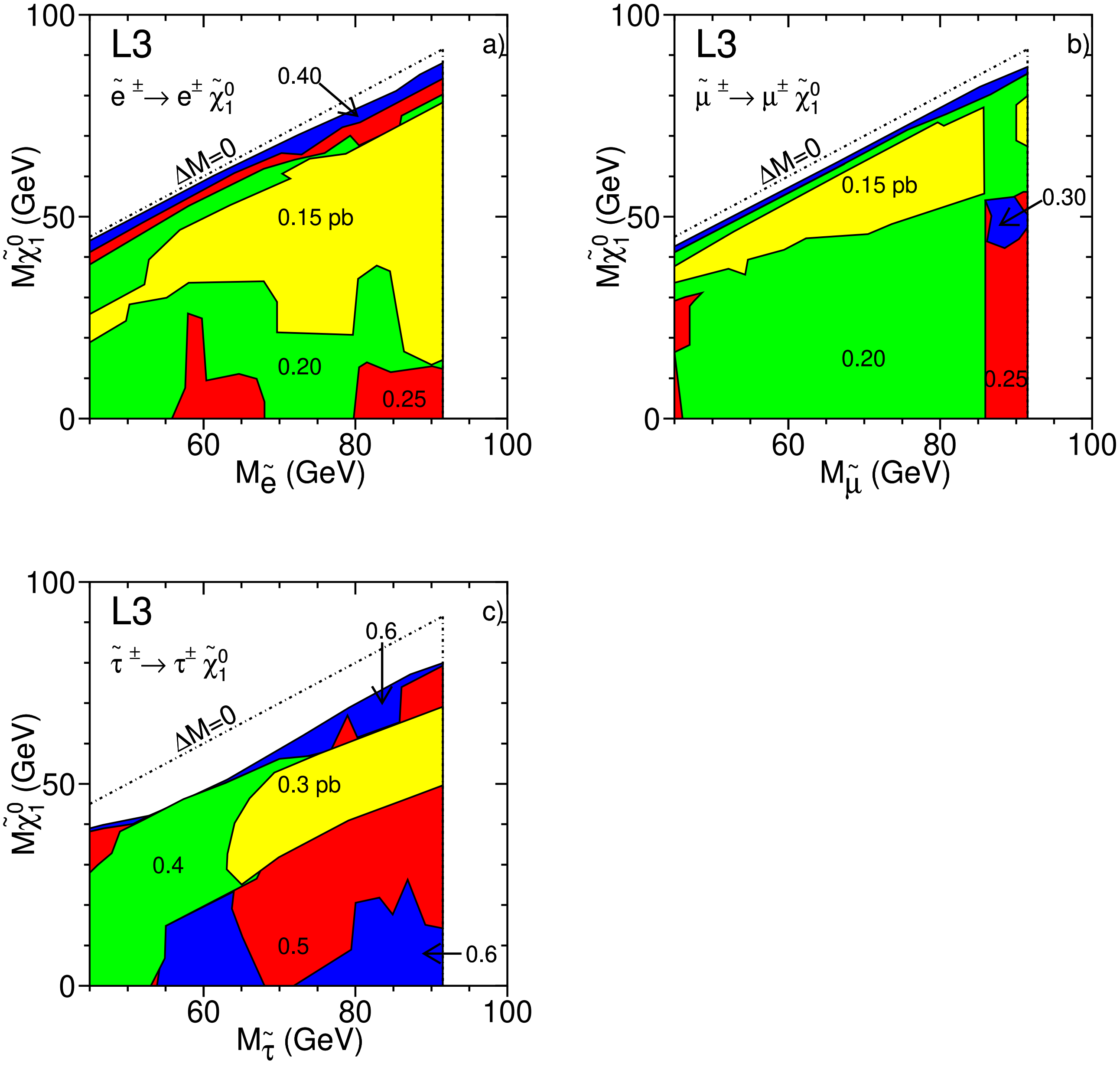

Figure 5: Model independent upper limits on production cross sections for scalar leptons in the plane $M_{\tilde{\chi}^0_1} - M_{\tilde{\ell}^\pm}$: a) scalar electrons, b) scalar muons and c) scalar taus. For all the limits the decay $\tilde{\ell}^\pm \to \ell^\pm \tilde{\chi}^0_1$ is assumed.

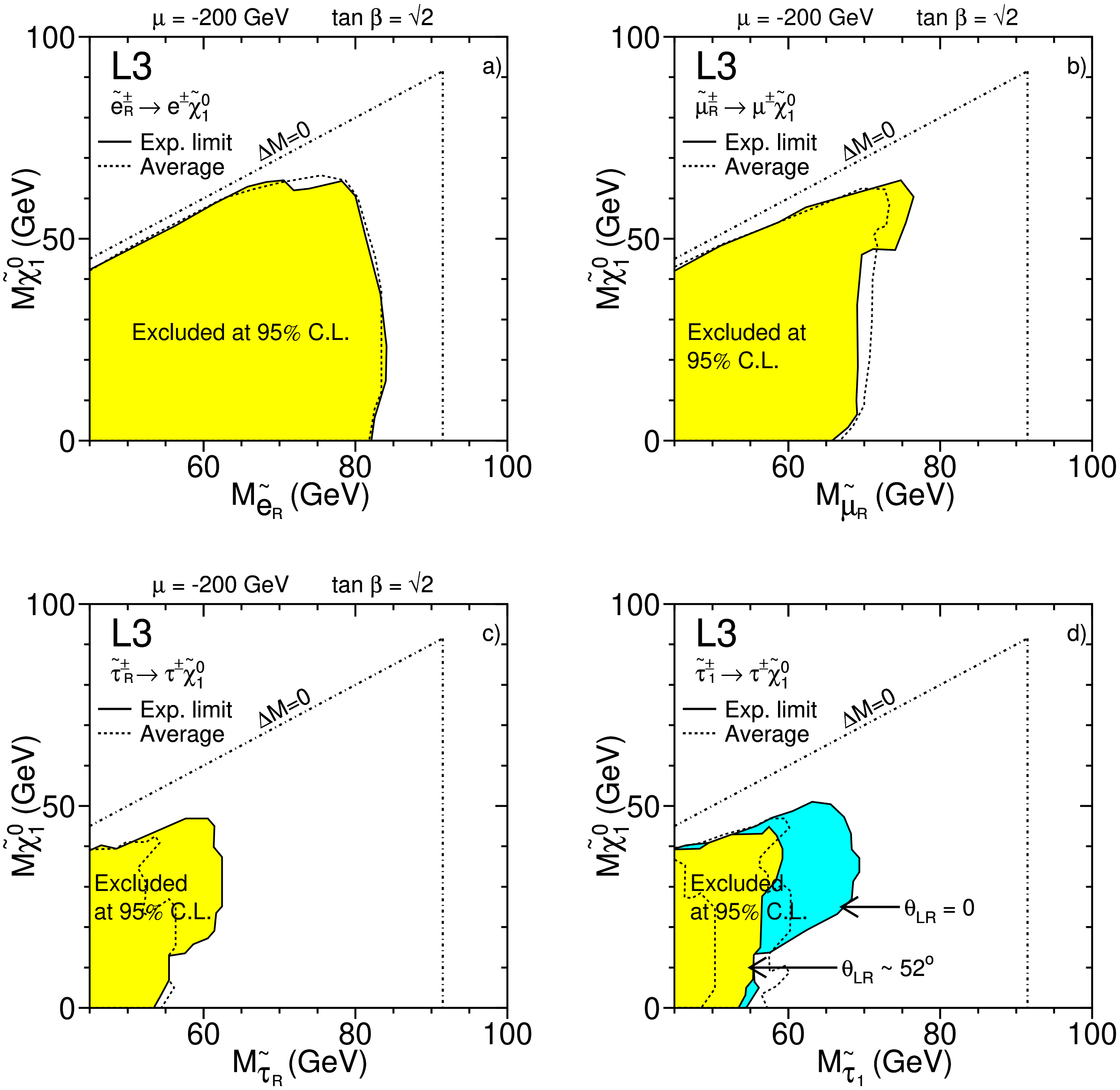

Figure 6: Mass limits on the scalar partners of right-handed a) electrons, b) muons and c) taus as a function of the neutralino mass, $M_{\tilde{\chi}^0_1}$. d) shows the exclusion for the scalar tau, when mixing between $\tilde{\tau}_R$ and $\tilde{\tau}_L$ occurs, for the minimal and maximal cross sections. These four exclusions are obtained using only the upper limits on the cross section obtained from direct searches at centre-of-mass energies between 130 GeV and 183 GeV. The dashed lines show the average limits obtained with Monte Carlo experiments with background only.

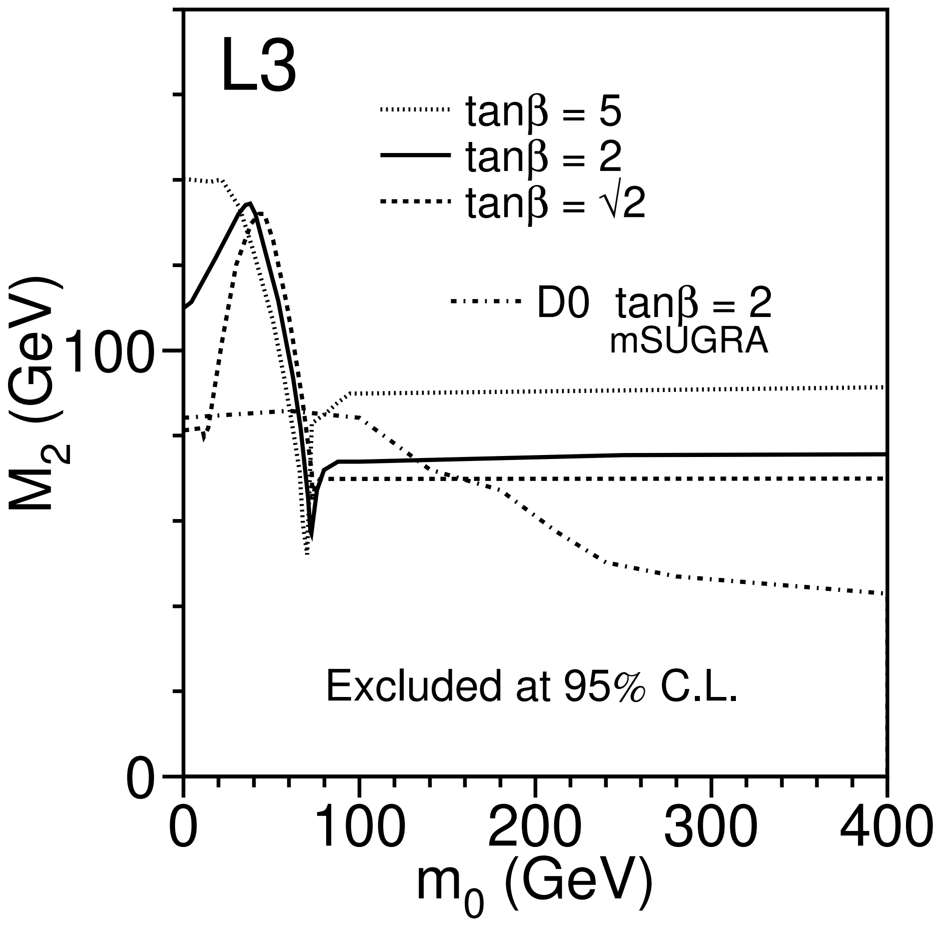

Figure 7: Exclusion domains in the $M_2 - m_0$ plane for several $\tan\beta$ values and for $\mu = -200$ GeV. Regions below the lines are excluded at 95% C.L. These exclusions are obtained by combining scalar electron and muon searches with the results of our search for charginos and neutralinos. The exclusion obtained by D0, at Tevatron, from a search for gluinos and scalar quarks in the mSUGRA framework [24] is also shown.